

# A QLP Decomposition via Randomization

Maboud F. Kaloorazi, J. Chen, and Rodrigo C. de Lamare

## Abstract

This paper is concerned with full matrix decomposition of matrices, primarily low-rank matrices. It develops a QLP-like decomposition algorithm such that when operating on a matrix  $\mathbf{A}$ , gives  $\mathbf{A} = \mathbf{QLP}^T$ , where  $\mathbf{Q}$  and  $\mathbf{P}$  are orthonormal, and  $\mathbf{L}$  is lower-triangular. The proposed algorithm, termed Rand-QLP, utilizes randomization and the unpivoted QR decomposition. This in turn enables Rand-QLP to leverage modern computational architectures, thus addressing a serious bottleneck associated with classical and most recent matrix decomposition algorithms. We derive several error bounds for Rand-QLP: bounds for the first  $k$  approximate singular values as well as the trailing block of the middle factor, which show that Rand-QLP is rank-revealing; and bounds for the distance between approximate subspaces and the exact ones for all four fundamental subspaces of a given matrix. We assess the speed and approximation quality of Rand-QLP on synthetic and real matrices with different dimensions and characteristics, and compare our results with those of multiple existing algorithms.

## Index Terms

Matrix decomposition, randomized rank-revealing factorization, communication-avoiding algorithm.

## I. INTRODUCTION

Matrix decomposition is a factorization of a matrix into simpler constituents. Matrix decompositions are powerful computational tools for solving a wide array of problems that appear in signal processing and machine learning applications. Their use is due to the fact that these applications require information about orthonormal bases for the row and/or column spaces of a matrix (the bases that span the four fundamental subspaces of the matrix), or the numerical

MF Kaloorazi (kaloorazi@xysu.edu.cn) is with the School of Electronic Engineering, Xi'an Shiyou University, Xi'an, China; J. Chen (jie.chen@nwpu.edu.cn) is with the School of Marine Science and Technology, Northwestern Polytechnical University, Xi'an, China; and RC de lamare (delamare@cetuc.puc-rio.br) is with the Centre for Telecommunications Studies, Pontifical Catholic University of Rio de Janeiro, Brazil.

rank, the condition number, or a low-rank representation of a matrix or a system. Applications of matrix decompositions include principal component analysis [1], least squares data fitting [2], matrix completion [3], image reconstruction [4], molecular dynamics simulations [5], sensor and multichannel signal processing [6], model matching for model order reduction [7], background modeling [8], vibrations of fluid-solid structures [9], subspace estimation over networks [10], seismic facies analysis for oil and gas reservoirs characterization [11], and IP networks anomaly detection [12].

The singular value decomposition (SVD) [13], the column-pivoted QR (CPQR), or rank-revealing QR factorization [14], the rank-revealing UTV decompositions [15]–[17], and the pivoted QLP (p-QLP) decomposition [18] are widely used to factor a general matrix. A major bottleneck associated with the computation of these factorizations is the communication cost [19]. This cost is prohibitive, makes execution of these algorithms on modern computers challenging and in turn stymies their application to large matrices. The communication cost [19] involves moving data between different levels of the memory hierarchy or/and between processors working in parallel. It is associated with the exploitation of level-1, 2 and 3 BLAS (the Basic Linear Algebra Subprograms) routines [20]–[24] by any algorithm: level-1 and level-2 BLAS routines are memory-bound and can not attain high performance on advanced architectures. Level-3 BLAS routines are, however, CPU-bound; they can harness the data locality in multi-core architectures, thus attaining higher performance, very close to that rendered by processors. Operations executed in level-3 BLAS can be 5 to 10 times faster than those executed in level-1 and level-2 BLAS.

**Our Contributions.** This work develops a matrix decomposition algorithm that uses randomization to construct an approximation to the SVD of a matrix. The decomposition takes the form of QLP and is called Rand-QLP. We derive error bounds for the approximate leading singular values and for the distance between all four approximate subspaces and the exact ones. The computation of Rand-QLP requires only matrix-matrix multiplication and the (unpivoted) QR decomposition and, as such, most of its operations are in level-3 BLAS. The Rand-QLP algorithm is simple, numerically stable, and can be coded using only a few lines of MATLAB code.

## II. RELATED WORK

Let  $\mathbf{A} \in \mathbb{R}^{m \times n}$ , with  $m \geq n$ , and its rank be  $k$ . The SVD is considered the best decomposition of a matrix, as it provides information on singular values and four fundamental subspaces of the

matrix. The (thin) SVD of  $\mathbf{A}$  is written as:

$$\mathbf{A} = \mathbf{U}\mathbf{\Sigma}\mathbf{V}^T = \begin{bmatrix} \mathbf{U}_k & \mathbf{U}_\perp \end{bmatrix} \begin{bmatrix} \mathbf{\Sigma}_k & \mathbf{0} \\ \mathbf{0} & \mathbf{\Sigma}_\perp \end{bmatrix} \begin{bmatrix} \mathbf{V}_k & \mathbf{V}_\perp \end{bmatrix}^T, \quad (1)$$

where  $\mathbf{U}_k \in \mathbb{R}^{m \times k}$  and  $\mathbf{U}_\perp \in \mathbb{R}^{m \times (n-k)}$  are orthonormal and span  $\mathcal{R}(\mathbf{A})$  and  $\mathcal{N}(\mathbf{A}^T)$ , respectively. The diagonal  $\mathbf{\Sigma} \in \mathbb{R}^{n \times n}$  contains the singular values  $\sigma_i$ s in a non-increasing order:  $\mathbf{\Sigma}_k$  comprises the first  $k$  and  $\mathbf{\Sigma}_\perp$  the remaining  $n-k$  singular values.  $\mathbf{V}_k \in \mathbb{R}^{n \times k}$  and  $\mathbf{V}_\perp \in \mathbb{R}^{n \times (n-k)}$  are orthonormal and span  $\mathcal{R}(\mathbf{A}^T)$  and  $\mathcal{N}(\mathbf{A})$ , respectively. ( $\mathcal{R}(\cdot)$  and  $\mathcal{N}(\cdot)$  indicate the range and null space.) The SVD can be used to determine the rank of a matrix, to compute angles between subspaces as well as optimal low-rank approximations.

The QR decomposition [13] gives  $\mathbf{A} = \mathbf{Q}_A \mathbf{R}_A$ , where  $\mathbf{Q}_A \in \mathbb{R}^{m \times n}$  is orthonormal and contains the bases for the columns of  $\mathbf{A}$ , and  $\mathbf{R}_A \in \mathbb{R}^{n \times n}$  is upper triangular. (This is in fact the “reduced” version of the decomposition, for silent columns and rows in the two factors were discarded [25].) A variant of the QR decomposition is the column-pivoted QR (CPQR), or rank-revealing QR decomposition [14]. It is computed by Householder orthogonal triangularization where columns with the largest magnitudes are swapped with other columns before the reduction proceeds. CPQR factors  $\mathbf{A}$  as:

$$\mathbf{A}\mathbf{\Pi} = \mathbf{Q}_{\text{piv}} \mathbf{R}_{\text{piv}} = \mathbf{Q}_{\text{piv}} \begin{bmatrix} \mathbf{R}_{11} & \mathbf{R}_{12} \\ \mathbf{0} & \mathbf{R}_{22} \end{bmatrix}, \quad (2)$$

where  $\mathbf{\Pi} \in \mathbb{R}^{n \times n}$  is a permutation matrix. CPQR is rank-revealing:  $\mathbf{R}_{11} \in \mathbb{R}^{k \times k}$  is well-conditioned with  $\sigma_{\min}(\mathbf{R}_{11}) = O(\sigma_k)$ , and  $\mathbf{R}_{22} \in \mathbb{R}^{(n-k) \times (n-k)}$  is sufficiently small, i.e.,  $\|\mathbf{R}_{22}\|_2 = O(\sigma_{k+1})$ . (Here  $\|\cdot\|_2$  indicates the  $\ell_2$ -norm.) Elements on the diagonal of  $\mathbf{R}_{\text{piv}}$  are approximations to singular values of  $\mathbf{A}$ . CPQR, however, does not explicitly establish orthonormal bases for the rows of  $\mathbf{A}$ .

Introduced by Stewart in [15] and [16], the rank-revealing URV and ULV decompositions are a compromise between the SVD and CPQR; they are more efficient than the SVD in terms of arithmetic cost, and they furnish orthonormal bases for  $\mathcal{R}(\mathbf{A}^T)$  and  $\mathcal{N}(\mathbf{A})$ . These algorithms, often called UTV decompositions, factor  $\mathbf{A}$  such as  $\mathbf{A} = \mathbf{U}\mathbf{T}\mathbf{V}^T$ ;  $\mathbf{U} \in \mathbb{R}^{m \times n}$  and  $\mathbf{V} \in \mathbb{R}^{n \times n}$  are orthonormal, and  $\mathbf{T} \in \mathbb{R}^{n \times n}$  is either upper triangular (the URV) or lower triangular (the ULV). Computation of UTV decompositions involves two main steps: an initial QR decomposition, and deflation steps to estimate the singular values [17], [26].

The pivoted QLP (p-QLP) decomposition is another rank-revealing algorithm [18]. It is built on CPQR: let  $\mathbf{A}$  have a CPQR such that  $\mathbf{A}\mathbf{\Pi} = \mathbf{Q}_{\text{piv}}\mathbf{R}_{\text{piv}}$ . Then a CPQR is performed on  $\mathbf{R}_{\text{piv}}^T$  such that  $\mathbf{R}_{\text{piv}}^T\mathbf{\Pi} = \mathbf{Q}'\mathbf{R}'$ . Hence p-QLP is given by:

$$\mathbf{A} = \mathbf{Q}_{\text{piv}}\mathbf{\Pi}\mathbf{R}'^T\mathbf{Q}'^T\mathbf{\Pi}^T \triangleq \mathbf{Q}_{\text{qlp}}\mathbf{L}\mathbf{P}^T.$$

$\mathbf{Q}_{\text{qlp}} \triangleq \mathbf{Q}_{\text{piv}}\mathbf{\Pi}$  and  $\mathbf{P} \triangleq \mathbf{\Pi}\mathbf{Q}'$  are orthonormal and contain bases for the columns and rows of  $\mathbf{A}$ , respectively, and diagonals of  $\mathbf{L} \triangleq \mathbf{R}'^T$  are approximations to the singular values of  $\mathbf{A}$ . (For other matrix decompositions see [2], [13].)

In order to compute the SVD of a matrix, the classical bidiagonalization method is usually used [13], [23], which comprises two main steps: reduction of the matrix to a bidiagonal form, and reduction of the bidiagonal form to a diagonal form. Most operations of these two steps are in level-1 and level-2 BLAS. Due to employment of the pivoting strategy, roughly half of the operations of CPQR are in BLAS-3 [27]. The UTV algorithm in the second step deflates large or small singular values one at a time [17], [26]. A large portion of these operations are in level-1 and level-2 BLAS. Most operations of the unpivoted QR decomposition are, however, in level-3 BLAS.

Recently, Nakatsukasa and Higham [28] developed the QR-based Dynamically Weighted Halley (QDWH)-SVD algorithm, a communication friendly algorithm for computing the SVD of a matrix. The building block of the algorithm is the computation of the polar decomposition [29], which is done by a Halley iteration using the QR decomposition. QDWH-SVD consists of two main steps: i) computation of the polar decomposition  $\mathbf{A} = \mathbf{U}_p\mathbf{H}$ , where  $\mathbf{U}_p \in \mathbb{R}^{m \times n}$  is orthonormal, and  $\mathbf{H} \in \mathbb{R}^{n \times n}$  is Hermitian positive semidefinite, and ii) computation of the eigendecomposition  $\mathbf{H} = \mathbf{V}\mathbf{\Sigma}\mathbf{V}^T$ . Hence  $\mathbf{A} = (\mathbf{U}_p\mathbf{V})\mathbf{\Sigma}\mathbf{V}^T$ . Martinsson, Quintana-Orti and Heavner [30] presented randUTV, a randomized algorithm that approximates the UTV decomposition of a matrix. Using randomization and the SVD, combined with power iteration technique and “oversampling”, randUTV factors one block of  $b$  columns of the matrix at a time. By piecing the results together, it constructs a UTV-like factorization of the matrix. A more detailed comparison of QDWH-SVD, randUTV and Rand-QLP in computational procedure, flop count and performance is given in Section V.

### III. PROPOSED RAND-QLP ALGORITHM

Matrix-matrix multiplication and the QR decomposition form the components of Rand-QLP computation. The algorithmic procedure of Rand-QLP for the matrix  $\mathbf{A}$  defined above is as

follows: a random matrix  $\Omega \in \mathbb{R}^{m \times n}$  (in this work standard Gaussian) is generated and left-multiplied by  $\mathbf{A}^T$ . Next, orthonormal bases for the columns of the matrix product are obtained, e.g., via the QR decomposition:

$$\bar{\mathbf{Q}} = \text{orth}(\mathbf{A}^T \Omega).$$

Then  $\bar{\mathbf{Q}} \in \mathbb{R}^{n \times n}$  is left-multiplied by  $\mathbf{A}$ , and orthonormal bases for the columns of the product  $\mathbf{A}\bar{\mathbf{Q}}$  are computed:

$$\mathbf{Q} = \text{orth}(\mathbf{A}\bar{\mathbf{Q}}).$$

We then form  $\mathbf{Q}^T \mathbf{A}$  and compute the QR decomposition of its transpose:

$$\mathbf{P}\mathbf{R} = (\mathbf{Q}^T \mathbf{A})^T.$$

Thus  $\mathbf{A} = \mathbf{Q}\mathbf{L}\mathbf{P}^T$ , where  $\mathbf{L} \triangleq \mathbf{R}^T$ . Algorithm 1 presents the procedure for computing Rand-QLP.

---

**Algorithm 1** Rand-QLP

---

**Input:** An  $m \times n$  matrix  $\mathbf{A}$ .

**Output:**  $\mathbf{Q} \in \mathbb{R}^{m \times n}$  is orthonormal and contains the approximate bases for  $\mathcal{R}(\mathbf{A})$  and  $\mathcal{N}(\mathbf{A}^T)$ ;  $\mathbf{L} \in \mathbb{R}^{n \times n}$  is lower triangular and its diagonals approximate the singular values;  $\mathbf{P} \in \mathbb{R}^{n \times n}$  is orthonormal and contains the approximate bases for  $\mathcal{R}(\mathbf{A}^T)$  and  $\mathcal{N}(\mathbf{A})$ .

- 1: **function**  $[\mathbf{Q}, \mathbf{L}, \mathbf{P}] = \text{Rand\_QLP}(\mathbf{A})$
  - 2:  $\Omega = \text{randn}(m, n)$
  - 3:  $\bar{\mathbf{Q}} = \text{orth}(\mathbf{A}^T \Omega)$
  - 4:  $\mathbf{Q} = \text{orth}(\mathbf{A}\bar{\mathbf{Q}})$
  - 5:  $\mathbf{P}\mathbf{R} = (\mathbf{Q}^T \mathbf{A})^T \rightarrow \mathbf{L} \triangleq \mathbf{R}^T$
  - 6: **end function**
- 

**Intuition.** To motivate the algorithm and to establish its error analysis, we first elaborate on the computation of p-QLP. Two CPQR decompositions are required to form p-QLP. However, as Stewart argues [18], the second CPQR is not necessary, due to column pivoting done by the first CPQR. In other words, if in the first step of the p-QLP computation a matrix  $\mathbf{Q}_{\text{piv}}$  is formed such that whose first  $k$  columns span  $\mathcal{R}(\mathbf{A})$  and whose last  $n - k$  columns span  $\mathcal{N}(\mathbf{A}^T)$ , as in (2), the second CPQR performed on  $\mathbf{R}_{\text{piv}}^T$  can then be supplanted by an unpivoted QR decomposition. In the computation of Rand-QLP, through right multiplication of  $\mathbf{A}^T$  by  $\Omega$  and of  $\mathbf{A}$  by  $\bar{\mathbf{Q}}$ , and

an orthonormalization thereafter, we construct a matrix  $\mathbf{Q}$  that gives a good approximation to  $\mathbf{Q}_{\text{piv}}$  in (2). The matrix  $\mathbf{Q}^T \mathbf{A}$  is in fact an approximation to  $\mathbf{R}_{\text{piv}}$ , and therefore we apply the QR decomposition to its transpose.

#### IV. ERROR BOUNDS AND COMPUTATIONAL COST

Let Rand-QLP compute a factorization for  $\mathbf{A}$  as follows:

$$\mathbf{A} = \mathbf{QLP}^T = [\mathbf{Q}_1 \quad \mathbf{Q}_2] \begin{bmatrix} \mathbf{L}_{11} & \mathbf{0} \\ \mathbf{L}_{21} & \mathbf{L}_{22} \end{bmatrix} \begin{bmatrix} \mathbf{P}_1^T \\ \mathbf{P}_2^T \end{bmatrix}, \quad (3)$$

where  $\mathbf{Q}_1 \in \mathbb{R}^{m \times k}$ ,  $\mathbf{Q}_2 \in \mathbb{R}^{m \times (n-k)}$ ,  $\mathbf{L}_{11} \in \mathbb{R}^{k \times k}$ ,  $\mathbf{L}_{22} \in \mathbb{R}^{(n-k) \times (n-k)}$ ,  $\mathbf{P}_1 \in \mathbb{R}^{n \times k}$ , and  $\mathbf{P}_2 \in \mathbb{R}^{n \times (n-k)}$ . Let further  $\mathbf{\Omega}_1 \in \mathbb{R}^{m \times k}$  be formed by the first  $k$  columns of the random matrix  $\mathbf{\Omega}$  used to compute Rand-QLP, and  $\tilde{\mathbf{\Omega}} \triangleq \mathbf{U}^T \mathbf{\Omega}_1 = [\tilde{\mathbf{\Omega}}_1^T \quad \tilde{\mathbf{\Omega}}_2^T]^T$ , where  $\tilde{\mathbf{\Omega}}_1 \in \mathbb{R}^{k \times k}$  and  $\tilde{\mathbf{\Omega}}_2 \in \mathbb{R}^{(n-k) \times k}$ . ( $\mathbf{U}$  contains  $\mathbf{A}$ 's left singular vectors.) The theorem below bounds the estimated leading singular values and off-diagonal block of  $\mathbf{L}$ , showing that Rand-QLP is rank-revealing. The proof is provided in the appendix.

*Theorem 1:* Let  $\mathbf{A}$  be an  $m \times n$  matrix whose SVD is defined in (1),  $\mathbf{L}$  be constructed by Rand-QLP whose diagonals are  $\hat{\sigma}_i$ , and  $\psi_i = \frac{\sigma_{k+1}}{\sigma_i}$ . Then, for  $i = 1, \dots, k$ , we have

$$\sigma_i \geq \hat{\sigma}_i \geq \frac{\sigma_i}{\sqrt{1 + \psi_i^4 \|\tilde{\mathbf{\Omega}}_2 \tilde{\mathbf{\Omega}}_1^{-1}\|_2^2}}. \quad (4)$$

$$\|\mathbf{L}_{22}\|_2 \leq \sigma_{k+1} + \frac{\psi_k^3 \sigma_1 \|\tilde{\mathbf{\Omega}}_2 \tilde{\mathbf{\Omega}}_1^{-1}\|_2}{\sqrt{1 + \psi_k^6 \|\tilde{\mathbf{\Omega}}_2 \tilde{\mathbf{\Omega}}_1^{-1}\|_2^2}}. \quad (5)$$

The distance between subspaces [13], denoted by  $\text{dist}()$ , is used to measure the closeness of two subspaces. It corresponds to the largest canonical angle between the subspaces. Let

$$\sin \theta_Q = \text{dist}(\mathcal{R}(\mathbf{U}_k), \mathcal{R}(\mathbf{Q}_1)).$$

$$\sin \phi_Q = \text{dist}(\mathcal{R}(\mathbf{U}_\perp), \mathcal{R}(\mathbf{Q}_2)).$$

$$\sin \theta_P = \text{dist}(\mathcal{R}(\mathbf{V}_k), \mathcal{R}(\mathbf{P}_1)).$$

$$\sin \phi_P = \text{dist}(\mathcal{R}(\mathbf{V}_\perp), \mathcal{R}(\mathbf{P}_2)).$$

The following theorem bounds the sine of canonical angles between all four estimated subspaces and the exact ones. The proof is given in the appendix.

*Theorem 2:* With the notation and hypotheses of Theorem 1, if  $\|\mathbf{L}_{22}\|_2 < \sigma_k(\mathbf{L}_{11})$  then

$$\sin\theta_Q \leq \psi_k^2 \|\tilde{\mathbf{\Omega}}_2 \tilde{\mathbf{\Omega}}_1^{-1}\|_2.$$

$$\sin\theta_P \leq \psi_k^3 \|\tilde{\mathbf{\Omega}}_2 \tilde{\mathbf{\Omega}}_1^{-1}\|_2.$$

$$\sin\phi_Q \leq \frac{\|\mathbf{L}_{22}\|_2^2}{\sigma_k^2(\mathbf{L}_{11}) - \|\mathbf{L}_{22}\|_2^2}.$$

$$\sin\phi_P \leq \|\mathbf{L}_{22}\|_2 / \sigma_k(\mathbf{L}_{11}).$$

**Computational Cost.** Computation of Rand-QLP requires the following flops (floating-point operations): generating the random matrix  $\mathbf{\Omega}$  needs  $mn$  flops; forming  $\mathbf{A}^T \mathbf{\Omega}$  needs  $2mn^2 - n^2$  flops, and orthonormalization of this matrix to obtain  $\bar{\mathbf{Q}}$  via the QR factorization needs  $5n^3/3$  flops; computing  $\mathbf{A}\bar{\mathbf{Q}}$  needs  $2mn^2 - mn$  flops; forming  $\mathbf{Q}$  needs  $2mn^2 - n^3/3$  flops; computing  $\mathbf{Q}^T \mathbf{A}$  requires  $2mn^2 - n^2$  flops, and the QR factorization on this matrix requires  $5n^3/3$  flops. Hence

$$C_{\text{Rand-QLP}} = 8mn^2 + 3n^3 - 2n^2.$$

The above cost involves computation of all approximate subspaces and singular vales of  $\mathbf{A}$  by Rand-QLP.

The cost of the SVD is comparable to that of Rand-QLP [13, p. 254]. Computing CPQR, however, requires  $2mn^2 + n^3 + 4(m^2n - mn^2)$  flops, which is around three times less that that of Rand-QLP. However, as pointed out earlier, computation of the SVD requires considerable amount of level-1 and level-2 BLAS operations [23], and only half of the flops of CPQR are in level-3 BLAS [27]. This makes implementation of these two algorithms challenging on advanced computers, as they can not be efficiently parallelized. However, Rand-QLP can be computed almost entirely using level-3 BLAS routines, thereby harnessing the parallel structure of modern computers.

## V. NUMERICAL SIMULATIONS

We conduct numerical tests to investigate the performance of Rand-QLP. The results are compared with those of multiple existing algorithms. Tests are done in MATLAB on a computer with a 1.8 GHz Intel Core i7 processor and 8 GB of memory.

### A. Runtime Comparison

We compare the speed of Rand-QLP against those of four algorithms, namely the SVD, CPQR, randUTV [30], and QDWH-SVD [28] (we discard p-QLP as its cost is over twice of that CPQR). Before presenting the runtime results, we discuss the last two algorithms in more detail.

- randUTV [30]. This algorithm uses randomized sampling and the SVD and gives a UTV-like factorization incrementally. The authors utilize the power iteration scheme and oversampling to improve the approximation accuracy. They argue that the cost of randUTV is three times higher than that of CPQR if the power iteration factor  $q$  is set to zero; if  $q = 1$  or  $q = 2$ , the cost would be four times or five times higher than that of CPQR, respectively. If a matrix  $\mathbf{A}$  is stored externally, randUTV needs two passes over  $\mathbf{A}$  if  $q = 0$ , and  $2q + 2$  passes over  $\mathbf{A}$  otherwise.
- QDWH-SVD [28]. To furnish the SVD for  $\mathbf{A}$ , this algorithm computes two polar decompositions, one for  $\mathbf{A}$  and one for  $\mathbf{H}$ , by using a Halley iteration. It performs the QR decomposition on matrices of size  $(m + n) \times n$  for  $\mathbf{A}$  and of size  $2n \times n$  for  $\mathbf{H}$ . The number of iterations can reach up to six, depending on the condition number [29] of  $\mathbf{A}$ . The flop count for QDWH-SVD ranges from  $8mn^2 + (27 + 2/3)n^3$  to  $24mn^2 + (28 + 1/3)n^3$ .

The flop counts for Rand-QLP and randUTV with  $q = 0$  are comparable. Further, the latter requires two passes over an externally stored  $\mathbf{A}$ , while the former needs three passes. However, randUTV with  $q \neq 0$  becomes computationally more demanding than Rand-QLP, as it needs more flops as well as passes over  $\mathbf{A}$ . Rand-QLP is more efficient than QDWH-SVD in computational cost.

**Synthetic Data.** We generate dense,  $n \times n$  matrices and apply the foregoing algorithms to decompose them. The runtime results are reported in Table I. For the SVD and CPQR, we used MATLAB `svd` and `qr` functions, and the results for randUTV and Rand-QLP were averaged over 10 runs.

We make several observations: Rand-QLP i) outperforms the SVD for all matrices; ii) begins to be more efficient than CPQR as the dimensions of the matrices grow; iii) is substantially faster than randUTV and QDWH-SVD; iv) and QDWH-SVD scale better than randUTV. If implemented on a highly parallel machine, we expect the gaps in runtime between Rand-QLP and the first two algorithms (the SVD and CPQR) to be larger in favor of Rand-QLP, and between Rand-QLP and the last two algorithms to be reduced. However, randUTV and QDWH-



SVD shall not be faster than Rand-QLP, because their computations require more arithmetic and communication costs.

**Real Data.** We select five sparse, square and non-symmetric matrices from the SuiteSparse Matrix Collection (formerly called the University of Florida Sparse Matrix Collection) [31] and decompose them via the considered algorithms. The runtime results are presented in Table II, which show that similar conclusions as those given above can be drawn.

TABLE I: Computational time (in seconds) for different algorithms on random matrices. For randUTV, we set the block size  $b=100$  and oversampling parameter to 5.

Algorithm	Dimension $n$					
	1000	2000	3000	4000	6000	8000
SVD	0.22	3.5	12.6	31.1	101	241
CPQR	0.06	1.3	5.5	12.6	41.4	99.9
randUTV (q=0)	0.49	11.6	52.9	156	643	1864
randUTV (q=2)	0.82	11.9	54.4	159	651	1876
QDWH-SVD	2.2	13.7	43.5	93.8	305	785
Rand-QLP	0.2	1.6	5.4	14.1	39.1	91.6

TABLE II: Computational time (in seconds) for different algorithms on real matrices from the SuiteSparse Matrix Collection.

Algorithm	watt1	meg1	gemat11	bayer03	goodwin
	n=1856	2904	4929	6747	7320
SVD	2.9	12.3	59.9	146	198
CPQR	1.1	5.3	24.6	89.5	104
randUTV (q=0)	9.2	58	323	1009	1601
randUTV (q=2)	9.6	59	328	1015	1646
QDWH-SVD	10.1	69	198	728	755
Rand-QLP	1.3	6.1	23.6	56.9	76.6

### B. Singular Values and Rank- $k$ Approximation

We construct a low-rank matrix perturbed with noise. It has one gap in the singular value spectrum and is formed as  $\mathbf{A} = \mathbf{U}\mathbf{\Sigma}\mathbf{V}^T + 0.05\sigma_k\mathbf{N}$ , where  $\mathbf{U}, \mathbf{V} \in \mathbb{R}^{n \times n}$  are random orthogonal matrices, and  $\mathbf{\Sigma} \in \mathbb{R}^{n \times n}$  is diagonal with entries  $\sigma_i$ s as singular values. The singular values

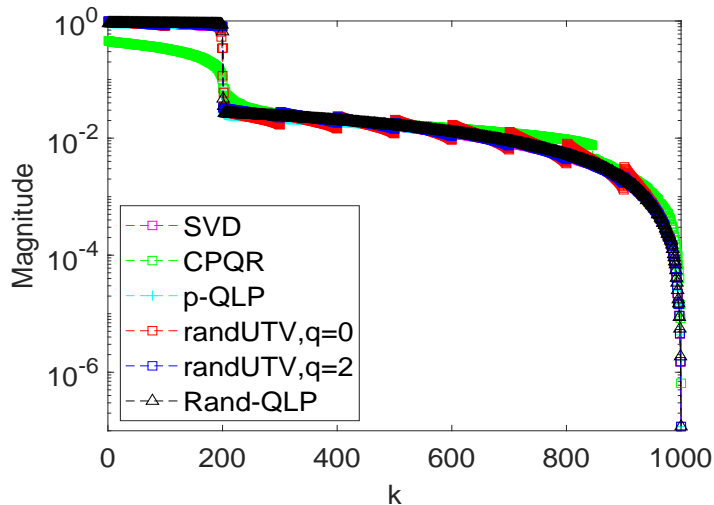


Fig. 1: Singular values approximation.

decrease linearly from 1 to  $10^{-20}$ , and we set  $\sigma_{k+1} = \dots = \sigma_n = 0$ . The matrix  $\mathbf{N}$  is normalized Gaussian. We set  $n = 1000$  and  $k = 200$ .

The results of approximating the singular values of  $\mathbf{A}$  are shown in Fig. 1. We observe that i) Rand-QLP strongly reveals the gap in the spectrum and provides approximations that are very close to those of p-QLP and the (optimal) SVD; ii) CPQR only suggests the gap; iii) randUTV with no power iteration ( $q = 0$ ) weakly reveals the rank and also introduces extra gaps in its approximations, and as such underestimates or overestimates most singular values. This result was expected: randUTV treats each block (of  $b$  columns) of an input matrix separately, and randomized algorithms tend to overestimate or/and underestimate singular values of a matrix if the power iteration is not used (see, e.g., [8]). In spite of improvement in approximation accuracy of randUTV by setting  $q = 2$ , the result suggests that a larger value of  $q$  is required for obtaining highly accurate approximations to the singular values. This in turn increases the cost of randUTV computation.

For the matrix  $\mathbf{A}$  above we compute rank- $k$  approximations by the algorithms considered; we vary  $k$  and compute the Frobenius error as  $\|\mathbf{A} - \widehat{\mathbf{A}}_k\|_F$ , where  $\widehat{\mathbf{A}}_k$  is a rank- $k$  approximation by either algorithm. The results are plotted in Fig. 2. We observe that i) Rand-QLP outperforms CPQR and randUTV with  $q = 0$ , and its approximation errors are very close to those incurred by p-QLP and the SVD; ii) the approximation errors by Rand-QLP and randUTV with  $q = 2$  are identical for  $k < 220$ , and the latter algorithm shows slightly better performance for a larger

$k$ . However, as expounded earlier, it demands more computational costs. We have provided in the appendix further results: the singular values and low-rank approximation results for two more matrices; and the singular values of the matrices of Table II computed by the considered algorithms.

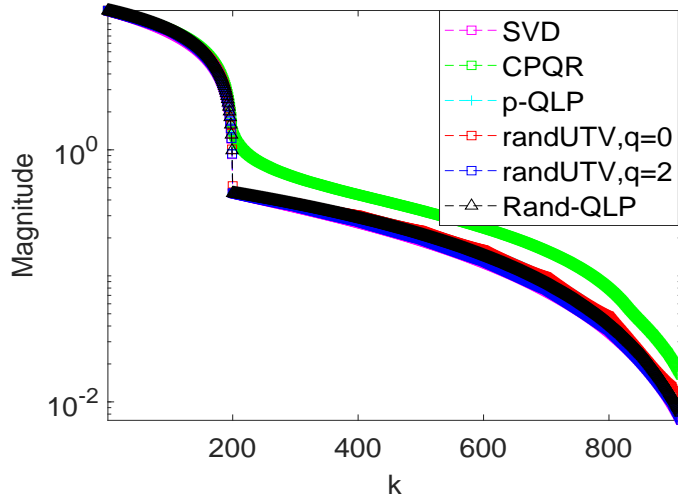


Fig. 2: Frobenius norm error for rank- $k$  approximation.

## VI. CONCLUSION

In this paper we presented Rand-QLP, a randomized rand-revealing algorithm that approximates the full SVD of a matrix. Its computation requires only matrix-matrix multiplication and the unpivoted QR factorization and can be done almost entirely using level-3 BLAS routines. Therefore, Rand-QLP can be efficiently parallelized on modern computational platforms. We furnished error bounds on i) the approximate leading singular values, ii) the angles between approximate four fundamental subspaces and the exact ones. We showed through numerical tests that Rand-QLP is faster than existing algorithms for large matrices, and that it provides approximations very close to those of p-QLP and the optimal SVD.

## VII. APPENDIX

This appendix provides the proofs for the results presented in Theorems 1 and 2. It also presents more experimental results on the approximation quality of Rand-QLP in relation to the state-of-the-art, demonstrating high-accuracy and robustness of Rand-QLP.

A. *Proof of Theorem 1, equation (4): bounds for the first  $k$  estimated singular values*

Let the matrix  $\mathbf{A}$  have a Rand-QLP decomposition as stated in equation (3). We have for the range of the matrix  $\mathbf{Q}$  in Step 4 of Algorithm 1:

$$\mathcal{R}(\mathbf{Q}) = \mathcal{R}(\mathbf{A}\bar{\mathbf{Q}}) = \mathcal{R}(\mathbf{A}\mathbf{A}^T\bar{\mathbf{\Omega}}). \quad (6)$$

Let matrices  $\mathbf{Q}$  and  $\bar{\mathbf{Q}}$  (Step 3 of Algorithm 1) be partitioned as follows:

$$\mathbf{Q} = [\mathbf{Q}_1 \quad \mathbf{Q}_2], \text{ and } \bar{\mathbf{Q}} = [\bar{\mathbf{Q}}_1 \quad \bar{\mathbf{Q}}_2], \quad (7)$$

where  $\mathbf{Q}_1$  and  $\bar{\mathbf{Q}}_1$  contain the first  $k$  columns of the corresponding matrices. Hence

$$\mathcal{R}(\mathbf{Q}_1) = \mathcal{R}(\mathbf{A}\bar{\mathbf{Q}}_1) = \mathcal{R}(\mathbf{A}\mathbf{A}^T\bar{\mathbf{\Omega}}_1). \quad (8)$$

Upon substitution of  $\mathbf{A}$  by its SVD, we obtain

$$\mathbf{A}\mathbf{A}^T\bar{\mathbf{\Omega}}_1 = \mathbf{U} \begin{bmatrix} \Sigma_k^2 \tilde{\mathbf{\Omega}}_1 \\ \Sigma_{\perp}^2 \tilde{\mathbf{\Omega}}_2 \end{bmatrix} = \ddot{\mathbf{Q}}\ddot{\mathbf{R}}. \quad (9)$$

We have  $\mathcal{R}(\mathbf{Q}_1) = \mathcal{R}(\ddot{\mathbf{Q}})$ , and both  $\tilde{\mathbf{\Omega}}_1$  and  $\tilde{\mathbf{\Omega}}_2$  have the standard Gaussian distribution due to the rotationally invariant property of  $\mathbf{\Omega}$ . We now define a  $k \times k$  matrix  $\mathbf{X} \triangleq \tilde{\mathbf{\Omega}}_1^{-1}\Sigma_k^{-2}$  and form the following matrix product on which a QR factorization is performed

$$\mathbf{A}\mathbf{A}^T\bar{\mathbf{\Omega}}_1\mathbf{X} = \mathbf{U} \begin{bmatrix} \mathbf{I}_k \\ \Sigma_{\perp}^2 \tilde{\mathbf{\Omega}}_2 \tilde{\mathbf{\Omega}}_1^{-1} \Sigma_k^{-2} \end{bmatrix} = \tilde{\mathbf{Q}}\tilde{\mathbf{R}}. \quad (10)$$

Let  $\mathbf{G} \triangleq \Sigma_{\perp}^2 \tilde{\mathbf{\Omega}}_2 \tilde{\mathbf{\Omega}}_1^{-1} \Sigma_k^{-2}$ , and

$$\mathbf{F}^{-1} \triangleq \tilde{\mathbf{R}}^{-1}\tilde{\mathbf{R}}^{-T} = (\tilde{\mathbf{R}}^T\tilde{\mathbf{R}})^{-1} = (\mathbf{I} + \mathbf{G}^T\mathbf{G})^{-1}. \quad (11)$$

Then, for  $\tilde{\mathbf{Q}}\tilde{\mathbf{Q}}^T$  we obtain

$$\tilde{\mathbf{Q}}\tilde{\mathbf{Q}}^T = \mathbf{U} \begin{bmatrix} \mathbf{F}^{-1} & \mathbf{F}^{-1}\mathbf{G}^T \\ \mathbf{G}\mathbf{F}^{-1} & \mathbf{G}\mathbf{F}^{-1}\mathbf{G}^T \end{bmatrix} \mathbf{U}^T. \quad (12)$$

By algebraic equivalency, we have

$$\mathbf{A}^T\mathbf{Q}_1 = \mathbf{P}_1\mathbf{L}_{11}^T, \quad (13)$$

and for  $i = 1, \dots, k$ ,  $\sigma_i(\mathbf{A}^T\mathbf{Q}_1) = \sigma_i(\mathbf{P}_1\mathbf{L}_{11}^T)$ . From  $\mathbf{I} \succeq \mathbf{Q}_1\mathbf{Q}_1^T$ , we have  $\mathbf{A}^T\mathbf{A} \succeq \mathbf{A}^T\mathbf{Q}_1\mathbf{Q}_1^T\mathbf{A}$ , which, by leveraging the Cauchy's interlacing theorem [32], gives

$$\lambda_i(\mathbf{A}^T\mathbf{A}) \geq \lambda_i(\mathbf{A}^T\mathbf{Q}_1\mathbf{Q}_1^T\mathbf{A}) = \lambda_i(\mathbf{A}^T\ddot{\mathbf{Q}}\ddot{\mathbf{Q}}^T\mathbf{A}) = \lambda_i(\mathbf{A}^T\tilde{\mathbf{Q}}\tilde{\mathbf{Q}}^T\mathbf{A}). \quad (14)$$

The last relation follows because for an orthogonal matrix  $\mathbf{W}$  of appropriate size, we have  $\ddot{\mathbf{Q}} = \tilde{\mathbf{Q}}\mathbf{W}$  (the same principle expresses the relation between  $\mathbf{Q}_1$  and  $\ddot{\mathbf{Q}}$ ). We obtain upon substitution

$$\mathbf{A}^T \tilde{\mathbf{Q}} \tilde{\mathbf{Q}}^T \mathbf{A} = \mathbf{V} \begin{bmatrix} \boldsymbol{\Sigma}_k \mathbf{F}^{-1} \boldsymbol{\Sigma}_k & \boldsymbol{\Sigma}_k \mathbf{F}^{-1} \mathbf{G}^T \boldsymbol{\Sigma}_\perp \\ \boldsymbol{\Sigma}_\perp \mathbf{G} \mathbf{F}^{-1} \boldsymbol{\Sigma}_k & \boldsymbol{\Sigma}_\perp \mathbf{G} \mathbf{F}^{-1} \mathbf{G}^T \boldsymbol{\Sigma}_k \end{bmatrix} \mathbf{V}^T. \quad (15)$$

Therefore

$$\lambda_i(\mathbf{A}^T \mathbf{A}) \geq \lambda_i(\mathbf{A}^T \tilde{\mathbf{Q}} \tilde{\mathbf{Q}}^T \mathbf{A}) \geq \lambda_i(\boldsymbol{\Sigma}_k \mathbf{F}^{-1} \boldsymbol{\Sigma}_k).$$

By applying the properties of partial ordering, it follows

$$\mathbf{G}^T \mathbf{G} \preceq \sigma_{k+1}^4 \|\tilde{\boldsymbol{\Omega}}_2 \tilde{\boldsymbol{\Omega}}_1^{-1}\|_2^2 \boldsymbol{\Sigma}_k^{-4} = \boldsymbol{\Psi}^4 \|\tilde{\boldsymbol{\Omega}}_2 \tilde{\boldsymbol{\Omega}}_1^{-1}\|_2^2,$$

where  $\boldsymbol{\Psi} = \text{diag}(\psi_1, \dots, \psi_k)$  is a  $k \times k$  matrix with entries  $\psi_i = \frac{\sigma_{k+1}}{\sigma_i}$ . Moreover

$$\boldsymbol{\Sigma}_k (\mathbf{I} + \mathbf{G}^T \mathbf{G})^{-1} \boldsymbol{\Sigma}_k \succeq \boldsymbol{\Sigma}_k (\mathbf{I} + \boldsymbol{\Psi}^4 \|\tilde{\boldsymbol{\Omega}}_2 \tilde{\boldsymbol{\Omega}}_1^{-1}\|_2^2)^{-1} \boldsymbol{\Sigma}_k,$$

which results in

$$\begin{aligned} \lambda_i(\mathbf{A}^T \mathbf{A}) &\geq \lambda_i(\mathbf{A}^T \tilde{\mathbf{Q}} \tilde{\mathbf{Q}}^T \mathbf{A}) \geq \lambda_i(\boldsymbol{\Sigma}_k (\mathbf{I} + \mathbf{G}^T \mathbf{G})^{-1} \boldsymbol{\Sigma}_k) \\ &\geq \frac{\sigma_i^2}{1 + \psi_i^4 \|\tilde{\boldsymbol{\Omega}}_2 \tilde{\boldsymbol{\Omega}}_1^{-1}\|_2^2}. \end{aligned}$$

The desired result follows by taking the square root of the last identity.

### B. Proof of Theorem 1, equation (5): bound for $\mathbf{L}_{22}$

Let

$$\bar{\mathbf{K}} \triangleq \mathbf{A}^T \mathbf{Q} = [\bar{\mathbf{K}}_1 \quad \bar{\mathbf{K}}_2] = [\mathbf{P}_1 \quad \mathbf{P}_2] \begin{bmatrix} \mathbf{L}_{11}^T & \mathbf{L}_{21}^T \\ \mathbf{0} & \mathbf{L}_{22}^T \end{bmatrix},$$

where  $\bar{\mathbf{K}}_1$  and  $\mathbf{P}_1$  contain the first  $k$  columns, and  $\bar{\mathbf{K}}_2$  and  $\mathbf{P}_2$  contain the remaining  $n - k$  columns of  $\bar{\mathbf{K}}$  and  $\mathbf{P}$ , respectively. Let

$$\mathbf{Z} \triangleq \mathbf{U}^T \mathbf{Q} = \begin{bmatrix} \mathbf{U}_k^T \\ \mathbf{U}_\perp^T \end{bmatrix} [\mathbf{Q}_1 \quad \mathbf{Q}_2] = \begin{bmatrix} \mathbf{Z}_{11} & \mathbf{Z}_{12} \\ \mathbf{Z}_{21} & \mathbf{Z}_{22} \end{bmatrix}.$$

With simple calculations (see, for example, [32, p. 13]), we will obtain the following equalities:

$$\bar{\mathbf{K}}_1 = \mathbf{P}_1 \mathbf{L}_{11}^T.$$

$$\bar{\mathbf{K}}_2 = \mathbf{V}_k \boldsymbol{\Sigma}_k \mathbf{Z}_{12} + \mathbf{V}_\perp \boldsymbol{\Sigma}_\perp \mathbf{Z}_{22}.$$

$$\mathbf{P}_{\bar{\mathbf{K}}_1^\perp} \bar{\mathbf{K}}_2 = \mathbf{P}_2 \mathbf{L}_{22}^T = (\mathbf{I} - \bar{\mathbf{K}}_1 \bar{\mathbf{K}}_1^{-1}) \bar{\mathbf{K}}_2 = (\mathbf{I} - \mathbf{P}_1 \mathbf{P}_1^T) \bar{\mathbf{K}}_2.$$

Hence

$$\|\mathbf{L}_{22}\|_2 \leq \|\mathbf{P}_2^T\|_2 \|(\mathbf{I} - \mathbf{P}_1 \mathbf{P}_1^T) \bar{\mathbf{K}}_2\|_2 \leq \|(\mathbf{I} - \mathbf{P}_1 \mathbf{P}_1^T) \bar{\mathbf{K}}_2\|_2.$$

Substituting  $\bar{\mathbf{K}}_2$  and applying the triangle inequality gives

$$\begin{aligned} \|\mathbf{L}_{22}\|_2 &\leq \|(\mathbf{I} - \mathbf{P}_1 \mathbf{P}_1^T) \mathbf{V}_k \Sigma_k \mathbf{Z}_{12}\|_2 + \|(\mathbf{I} - \mathbf{P}_1 \mathbf{P}_1^T) \mathbf{V}_\perp \Sigma_\perp \mathbf{Z}_{22}\|_2 \\ &= \|(\mathbf{I} - \mathbf{P}_1 \mathbf{P}_1^T) \mathbf{A}_k^T\|_2 + \|(\mathbf{I} - \mathbf{P}_1 \mathbf{P}_1^T) \mathbf{V}_\perp \Sigma_\perp\|_2, \end{aligned} \quad (16)$$

where  $\mathbf{A}_k^T \triangleq \mathbf{U}_k \Sigma_k \mathbf{V}_k^T$ . For the second term on the right-hand side of (16), we get

$$\|(\mathbf{I} - \mathbf{P}_1 \mathbf{P}_1^T) \mathbf{V}_\perp \Sigma_\perp\|_2 \leq \|(\mathbf{I} - \mathbf{P}_1 \mathbf{P}_1^T)\|_2 \|\mathbf{V}_\perp\|_2 \|\Sigma_\perp\|_2 \leq \sigma_{k+1}. \quad (17)$$

We have for the range of the matrix  $\mathbf{P}$  in Step 5 of Algorithm 1:

$$\mathcal{R}(\mathbf{P}) = \mathcal{R}(\mathbf{A}^T \mathbf{Q}) = \mathcal{R}(\mathbf{A}^T \mathbf{A} \bar{\mathbf{Q}}) = \mathcal{R}(\mathbf{A}^T \mathbf{A} \mathbf{A}^T \Omega).$$

Thus

$$\mathcal{R}(\mathbf{P}_1) = \mathcal{R}(\mathbf{A}^T \mathbf{Q}_1) = \mathcal{R}(\mathbf{A}^T \mathbf{A} \bar{\mathbf{Q}}_1) = \mathcal{R}(\mathbf{A}^T \mathbf{A} \mathbf{A}^T \Omega_1).$$

Defining a  $k \times k$  matrix  $\bar{\mathbf{X}} \triangleq \tilde{\Omega}_1^{-1} \Sigma_k^{-3}$  and performing a QR factorization on  $\mathbf{A}^T \mathbf{A} \mathbf{A}^T \Omega_1 \bar{\mathbf{X}}$  gives

$$\mathbf{A}^T \mathbf{A} \mathbf{A}^T \Omega_1 \bar{\mathbf{X}} = \mathbf{V} \begin{bmatrix} \mathbf{I}_k \\ \Sigma_\perp^3 \tilde{\Omega}_2 \tilde{\Omega}_1^{-1} \Sigma_k^{-3} \end{bmatrix} = \mathring{\mathbf{Q}} \mathring{\mathbf{R}}. \quad (18)$$

Let  $\bar{\mathbf{G}} = \Sigma_\perp^3 \tilde{\Omega}_2 \tilde{\Omega}_1^{-1} \Sigma_k^{-3}$ , and

$$\bar{\mathbf{F}}^{-1} \triangleq \mathring{\mathbf{R}}^{-1} \mathring{\mathbf{R}}^{-T} = (\mathring{\mathbf{R}}^T \mathring{\mathbf{R}})^{-1} = (\mathbf{I} + \bar{\mathbf{G}}^T \bar{\mathbf{G}})^{-1}.$$

Thus

$$\mathring{\mathbf{Q}} \mathring{\mathbf{Q}}^T = \mathbf{V} \begin{bmatrix} \bar{\mathbf{F}}^{-1} & \bar{\mathbf{F}}^{-1} \bar{\mathbf{G}}^T \\ \bar{\mathbf{G}} \bar{\mathbf{F}}^{-1} & \bar{\mathbf{G}} \bar{\mathbf{F}}^{-1} \bar{\mathbf{G}}^T \end{bmatrix} \mathbf{V}^T.$$

Since  $\mathbf{P}_1 \mathbf{P}_1^T = \mathring{\mathbf{Q}} \mathring{\mathbf{Q}}^T$ , we get

$$\mathbf{I} - \mathbf{P}_1 \mathbf{P}_1^T = \mathbf{I} - \mathring{\mathbf{Q}} \mathring{\mathbf{Q}}^T = \mathbf{V} \begin{bmatrix} \mathbf{I} - \bar{\mathbf{F}}^{-1} & \bar{\mathbf{F}}^{-1} \bar{\mathbf{G}}^T \\ -\bar{\mathbf{G}} \bar{\mathbf{F}}^{-1} & \mathbf{I} - \bar{\mathbf{G}} \bar{\mathbf{F}}^{-1} \bar{\mathbf{G}}^T \end{bmatrix} \mathbf{V}^T.$$

Writing  $\mathbf{A}_k^T = \mathbf{V} [\Sigma_k \quad \mathbf{0}; \mathbf{0} \quad \mathbf{0}] \mathbf{U}^T$ , we obtain

$$(\mathbf{I} - \mathbf{P}_1 \mathbf{P}_1^T) \mathbf{A}_k^T = \mathbf{V} \begin{bmatrix} (\mathbf{I} - \bar{\mathbf{F}}^{-1}) \Sigma_k \\ -\bar{\mathbf{G}} \bar{\mathbf{F}}^{-1} \Sigma_k \end{bmatrix} \mathbf{U}^T.$$

It follows that

$$\begin{aligned} \|(\mathbf{I} - \mathbf{P}_1 \mathbf{P}_1^T) \mathbf{A}_k^T\|_2^2 &= \|\boldsymbol{\Sigma}_k (\mathbf{I} - \bar{\mathbf{F}}^{-1}) \boldsymbol{\Sigma}_k\|_2 \\ &\leq \|\boldsymbol{\Sigma}_k\|_2^2 \|\mathbf{I} - \bar{\mathbf{F}}^{-1}\|_2, \end{aligned} \quad (19)$$

where we have used the following relation that holds for any matrix  $\mathbf{A}$  with  $\mathbf{I} + \mathbf{A}$  being non-singular [33]:

$$(\mathbf{I} + \mathbf{A})^{-1} = \mathbf{I} - \mathbf{A}(\mathbf{I} + \mathbf{A})^{-1} = \mathbf{I} - (\mathbf{I} + \mathbf{A})^{-1} \mathbf{A}.$$

The matrix  $\mathbf{I} - \bar{\mathbf{F}}^{-1}$  is positive semidefinite, and its eigenvalues satisfy [32, p. 148]:

$$\lambda_i(\mathbf{I} - \bar{\mathbf{F}}^{-1}) = \frac{\sigma_i^2(\bar{\mathbf{G}})}{1 + \sigma_i^2(\bar{\mathbf{G}})}, \quad i = 1, \dots, k.$$

The largest singular value of  $\bar{\mathbf{G}}$  satisfies:

$$\sigma_1(\bar{\mathbf{G}}) \leq \psi_k^3 \|\tilde{\boldsymbol{\Omega}}_2 \tilde{\boldsymbol{\Omega}}_1^{-1}\|_2.$$

Accordingly,

$$\lambda_1(\mathbf{I} - \bar{\mathbf{F}}^{-1}) \leq \frac{\psi_k^6 \|\tilde{\boldsymbol{\Omega}}_{21} \tilde{\boldsymbol{\Omega}}_{11}^{-1}\|_2^2}{1 + \psi_k^6 \|\tilde{\boldsymbol{\Omega}}_2 \tilde{\boldsymbol{\Omega}}_1^{-1}\|_2^2}.$$

Plugging this result into (19) and taking the square root, combined with (17) gives the desired result.

### C. Proof of Theorem 2: upper bounds for the sines of canonical angles

*Upper bound for  $\sin\theta_Q$ .* According to Theorem 2.6.1 of [13] we have

$$\begin{aligned} \sin\theta_Q &= \|\mathbf{U}_\perp^T \mathbf{Q}_1\|_2 = \|\mathbf{U}_k \mathbf{U}_k^T - \mathbf{Q}_1 \mathbf{Q}_1^T\|_2 \\ &= \|\mathbf{U}_k \mathbf{U}_k^T - \tilde{\mathbf{Q}} \tilde{\mathbf{Q}}^T\|_2 = \|\mathbf{U}_\perp^T \tilde{\mathbf{Q}}\|_2. \end{aligned}$$

The first relation in the second line follows due to  $\mathbf{Q}_1 \mathbf{Q}_1^T = \tilde{\mathbf{Q}} \tilde{\mathbf{Q}}^T$ , as shown before. Writing (10) as:

$$\begin{bmatrix} \mathbf{I}_k \\ \boldsymbol{\Sigma}_\perp^2 \tilde{\boldsymbol{\Omega}}_2 \tilde{\boldsymbol{\Omega}}_1^{-1} \boldsymbol{\Sigma}_k^{-2} \end{bmatrix} = \begin{bmatrix} \mathbf{U}_k^T \\ \mathbf{U}_\perp^T \end{bmatrix} \tilde{\mathbf{Q}} \tilde{\mathbf{R}},$$

it follows  $\tilde{\mathbf{R}}^{-1} = \mathbf{U}_k^T \tilde{\mathbf{Q}}$ , and hence

$$\mathbf{U}_\perp^T \tilde{\mathbf{Q}} = \boldsymbol{\Sigma}_\perp^2 \tilde{\boldsymbol{\Omega}}_2 \tilde{\boldsymbol{\Omega}}_1^{-1} \boldsymbol{\Sigma}_k^{-2} \mathbf{U}_k \tilde{\mathbf{Q}}.$$

Therefore

$$\sin\theta_Q = \|\mathbf{U}_\perp^T \tilde{\mathbf{Q}}\|_2 \leq \|\boldsymbol{\Sigma}_\perp^2 \tilde{\boldsymbol{\Omega}}_2 \tilde{\boldsymbol{\Omega}}_1^{-1} \boldsymbol{\Sigma}_k^{-2}\|_2 \|\mathbf{U}_k \tilde{\mathbf{Q}}\|_2 \leq \psi_k^2 \|\boldsymbol{\Omega}_2 \boldsymbol{\Omega}_1^{-1}\|_2.$$

Upper bound for  $\sin\theta_P$ .  $\sin\theta_P$  is defined as follows:

$$\begin{aligned}\sin\theta_P &= \|\mathbf{V}_\perp^T \mathbf{P}_1\|_2 = \|\mathbf{V}_k \mathbf{V}_k^T - \mathbf{P}_1 \mathbf{P}_1^T\|_2 \\ &= \|\mathbf{V}_k \mathbf{V}_k^T - \mathring{\mathbf{Q}} \mathring{\mathbf{Q}}^T\|_2 = \|\mathbf{V}_\perp^T \mathring{\mathbf{Q}}\|_2.\end{aligned}$$

The first relation in the second line follows because  $\mathbf{P}_1 \mathbf{P}_1^T = \mathring{\mathbf{Q}} \mathring{\mathbf{Q}}^T$ . From (18), we get  $\mathring{\mathbf{R}}^{-1} = \mathbf{V}_k^T \mathring{\mathbf{Q}}$ . Henec

$$\sin\theta_P = \|\mathbf{V}_\perp^T \mathring{\mathbf{Q}}\|_2 = \|\Sigma_\perp^3 \tilde{\Omega}_2 \tilde{\Omega}_1^{-1} \Sigma_k^{-3} \mathbf{V}_k \mathring{\mathbf{Q}}\|_2 \leq \psi_k^3 \|\Omega_2 \Omega_1^{-1}\|_2.$$

Upper bound for  $\sin\phi_Q$ . Assumption:  $\|\mathbf{L}_{22}\|_2 < \sigma_k(\mathbf{L}_{11})$ . A rank- $k$  approximation  $\hat{\mathbf{A}}_k$  of  $\mathbf{A}$  by Rand-QLP is given by

$$\hat{\mathbf{A}}_k = \mathbf{Q} \begin{bmatrix} \mathbf{L}_{11} \\ \mathbf{L}_{21} \end{bmatrix} \mathbf{P}_1^T = \hat{\mathbf{U}} \hat{\Sigma} \hat{\mathbf{V}}^T,$$

where orthonormal  $\hat{\mathbf{U}} \in \mathbb{R}^{m \times k}$  and  $\hat{\mathbf{V}} \in \mathbb{R}^{n \times k}$  and diagonal  $\hat{\Sigma} \in \mathbb{R}^{k \times k}$  are the SVD components. Note that  $\sin\phi_Q = \|\hat{\mathbf{U}}^T \mathbf{U}_\perp\|_2$ . We have

$$\begin{aligned}\hat{\mathbf{U}}^T \mathbf{U}_\perp &= \hat{\Sigma}^{-1} \hat{\mathbf{V}}^T \hat{\mathbf{A}}_k^T \mathbf{U}_\perp = \hat{\Sigma}^{-1} \hat{\mathbf{V}}^T \mathbf{P}_1 \mathbf{P}_1^T \mathbf{A}^T \mathbf{U}_\perp \\ &= \hat{\Sigma}^{-1} \hat{\mathbf{V}}^T \mathbf{P}_1 \mathbf{P}_1^T \mathbf{V}_\perp \Sigma_\perp = \hat{\Sigma}^{-1} \hat{\mathbf{V}}^T \mathbf{V}_\perp \Sigma_\perp.\end{aligned}$$

The last relation follows because there is an orthogonal matrix  $\mathbf{Y}$  for which  $\hat{\mathbf{V}} = \mathbf{P}_1 \mathbf{Y}$ , and hence  $\hat{\mathbf{V}} \hat{\mathbf{V}}^T = \mathbf{P}_1 \mathbf{P}_1^T$ . We have

$$\begin{aligned}\hat{\mathbf{V}}^T \mathbf{V}_\perp &= \hat{\Sigma}^{-1} \hat{\mathbf{U}}^T \hat{\mathbf{A}}_k \mathbf{V}_\perp = \hat{\Sigma}^{-1} \hat{\mathbf{U}}^T [\mathbf{A} - \mathbf{Q}_2 \mathbf{L}_{22} \mathbf{P}_2^T] \mathbf{V}_\perp \\ &= \hat{\Sigma}^{-1} \hat{\mathbf{U}}^T \mathbf{U}_\perp \Sigma_\perp - \hat{\Sigma}^{-1} \hat{\mathbf{U}}^T \mathbf{Q}_2 \mathbf{L}_{22} \mathbf{P}_2^T \mathbf{V}_\perp.\end{aligned}$$

Thus

$$\begin{aligned}\hat{\mathbf{U}}^T \mathbf{U}_\perp &= \hat{\Sigma}^{-1} \hat{\mathbf{V}}^T \mathbf{V}_\perp \Sigma_\perp \\ &= \hat{\Sigma}^{-2} \hat{\mathbf{U}}^T \mathbf{U}_\perp \Sigma_\perp^2 - \hat{\Sigma}^{-2} \hat{\mathbf{U}}^T \mathbf{Q}_2 \mathbf{L}_{22} \mathbf{P}_2^T \mathbf{V}_\perp \Sigma_\perp.\end{aligned}$$

Accordingly

$$\begin{aligned}\sin\phi_Q &\leq \|\hat{\Sigma}^{-1}\|_2^2 \|\Sigma_\perp^2\|_2 \sin\phi_Q + \|\hat{\Sigma}^{-1}\|_2^2 \|\mathbf{L}_{22}\|_2 \|\Sigma_\perp^2\|_2 \\ &\leq \frac{\|\mathbf{L}_{22}\|_2^2 / \sigma_k^2(\mathbf{L}_{11})}{1 - \|\mathbf{L}_{22}\|_2^2 / \sigma_k^2(\mathbf{L}_{11})}.\end{aligned}$$

This is the desired result since  $\hat{\sigma}_k \geq \sigma_k(\mathbf{L}_{11})$  and  $\|\mathbf{L}_{22}\|_2 = \sigma_1(\mathbf{L}_{22}) \geq \sigma_{k+1}$ .



*Upper bound for  $\sin\phi_P$ .* Noting that  $\sin\phi_P = \|\mathbf{V}_k^T \mathbf{P}_2\|_2$ , and writing  $\mathbf{A} = \mathbf{A}_k + \mathbf{A}_\perp = \mathbf{U}_k \boldsymbol{\Sigma}_k \mathbf{V}_k^T + \mathbf{U}_\perp \boldsymbol{\Sigma}_\perp \mathbf{V}_\perp^T$ , we then have

$$\begin{aligned} \sin\phi_P &= \|\mathbf{V}_k^T \mathbf{P}_2\|_2 = \|\boldsymbol{\Sigma}_k^{-1} \mathbf{U}_k^T \mathbf{A} \mathbf{P}_2\|_2 \\ &= \|\boldsymbol{\Sigma}_k^{-1} \mathbf{U}_k^T \mathbf{Q} \begin{bmatrix} \mathbf{L}_{11} & \mathbf{0} \\ \mathbf{L}_{21} & \mathbf{L}_{22} \end{bmatrix} \begin{bmatrix} \mathbf{P}_1^T \\ \mathbf{P}_2^T \end{bmatrix}\|_2 \\ &\leq \|\boldsymbol{\Sigma}_k^{-1}\|_2 \|\mathbf{L}_{22}\|_2 \\ &\leq \|\mathbf{L}_{22}\|_2 / \sigma_k(\mathbf{L}_{11}). \end{aligned}$$

#### D. Results on singular values and rank- $k$ approximation

We construct two square matrices of order  $n = 1000$  formed as  $\mathbf{A} = \mathbf{U}\boldsymbol{\Sigma}\mathbf{V}^T$ , where  $\mathbf{U}, \mathbf{V} \in \mathbb{R}^{n \times n}$  are random orthogonal matrices, and  $\boldsymbol{\Sigma} \in \mathbb{R}^{n \times n}$  is a diagonal matrix with entries  $\sigma_i$ s as singular values (similar matrices have been used in [30]):

- Fast decay. Decaying relatively fast, the entries of  $\boldsymbol{\Sigma}$  of this matrix take the form  $\sigma_i = i^{-2}$  for  $i = 1, \dots, n$ .
- S-shaped decay. The entries of  $\boldsymbol{\Sigma}$  of this matrix hover around 1, then decay quickly, and finally level out at 0.01.

Figures 3 and 4 show the estimated singular values for the above two matrices, and Figures 5-9 show the rank- $k$  approximation errors: Figures 5 and 6 demonstrate the Frobenius-norm errors, while Figures 7-9 demonstrate the  $\ell_2$  (or) spectral norm errors. Figures 10-14 show the computed singular values for the five sparse matrices from the SuiteSparse Matrix Collection.

We observe that (i) in Figure 3, Rand-QLP outperforms CPQR and randUTV and produces singular values as accurate as those of p-QLP and the optimal SVD; (ii) in Figure 4, the approximations by Rand-QLP are better than those of CPQR and are very close to p-QLP and the SVD; in Figures 5 and 6, the errors incurred by Rand-QLP match those of p-QLP and the SVD; in Figures 7-9, the errors generated by Rand-QLP are less than those of CPQR, are as good as those of p-QLP and are comparable to randUTV; in Figures 10-14 provides singular values as accurate as those of p-QLP and the optimal SVD.

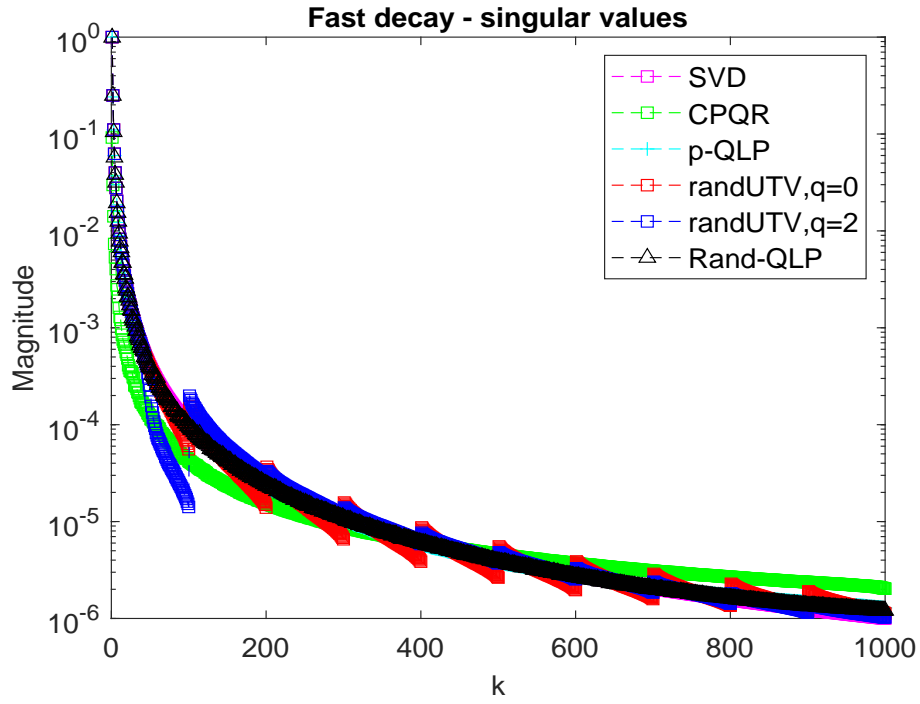


Fig. 3: Singular values approximation.

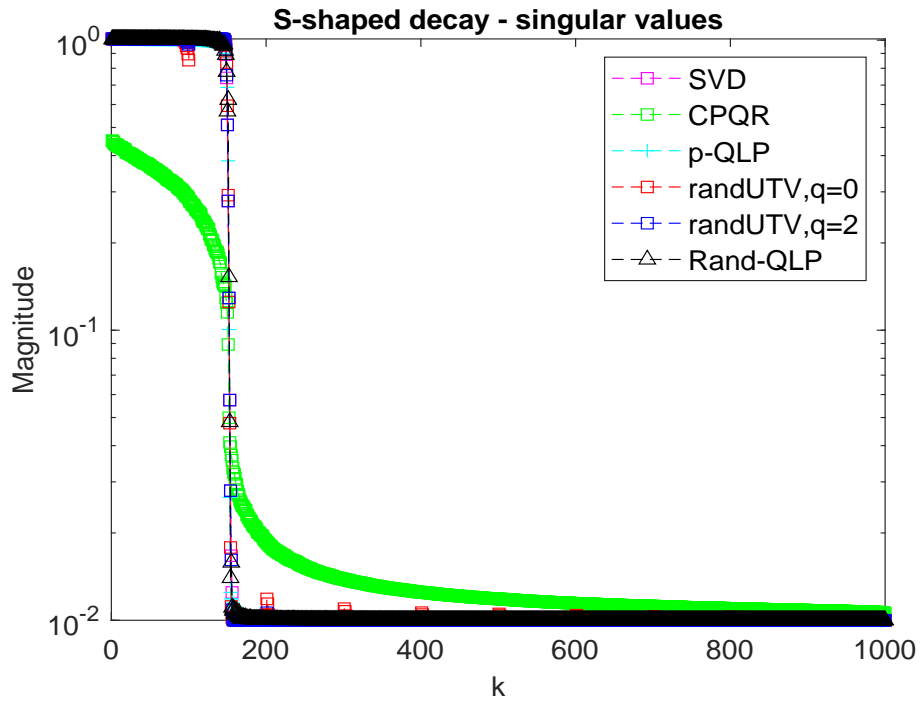
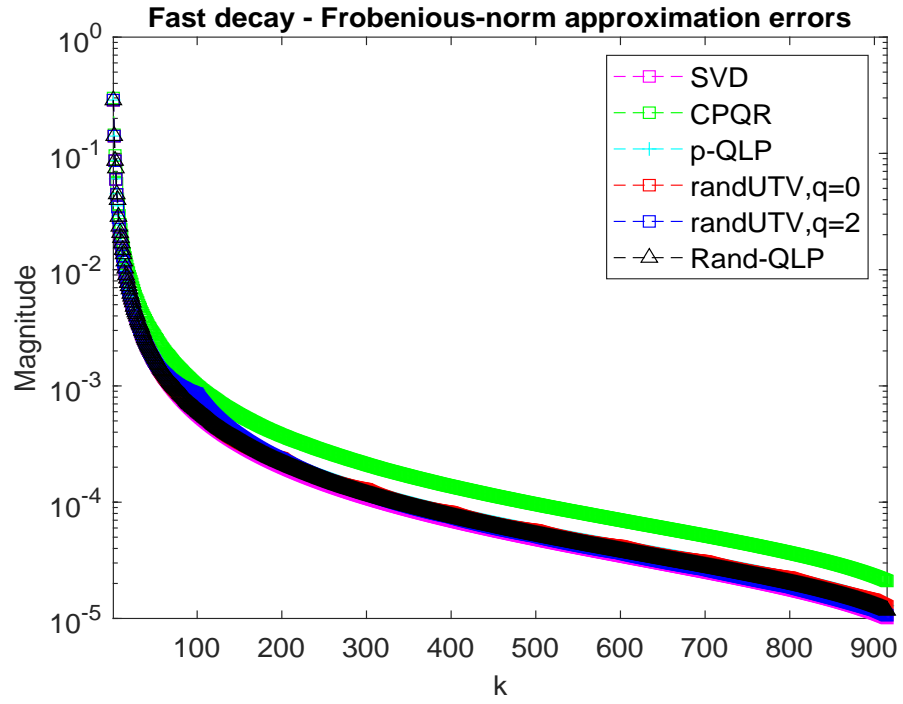
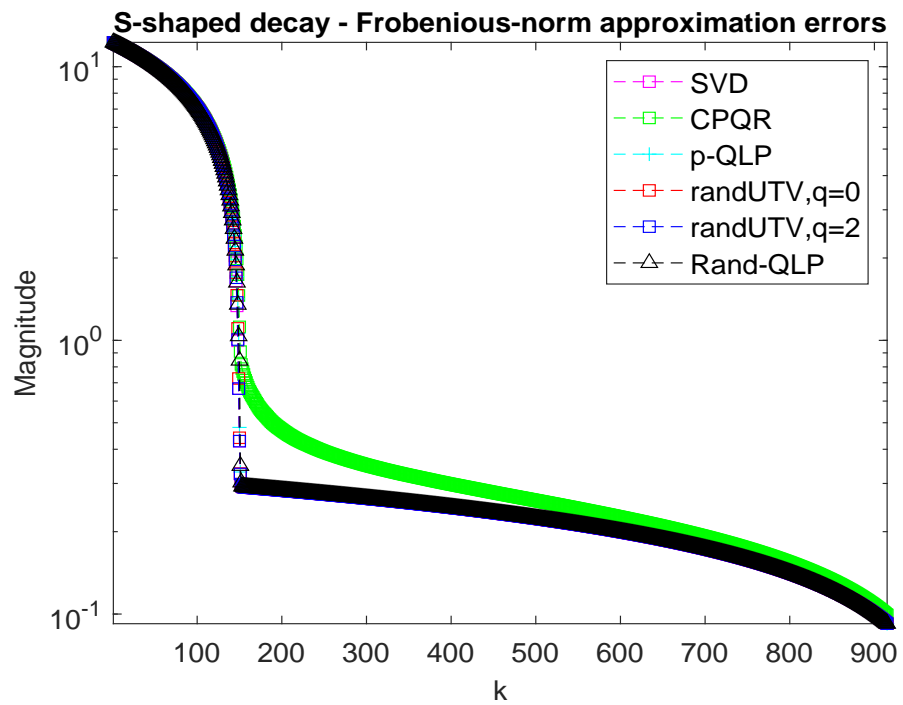
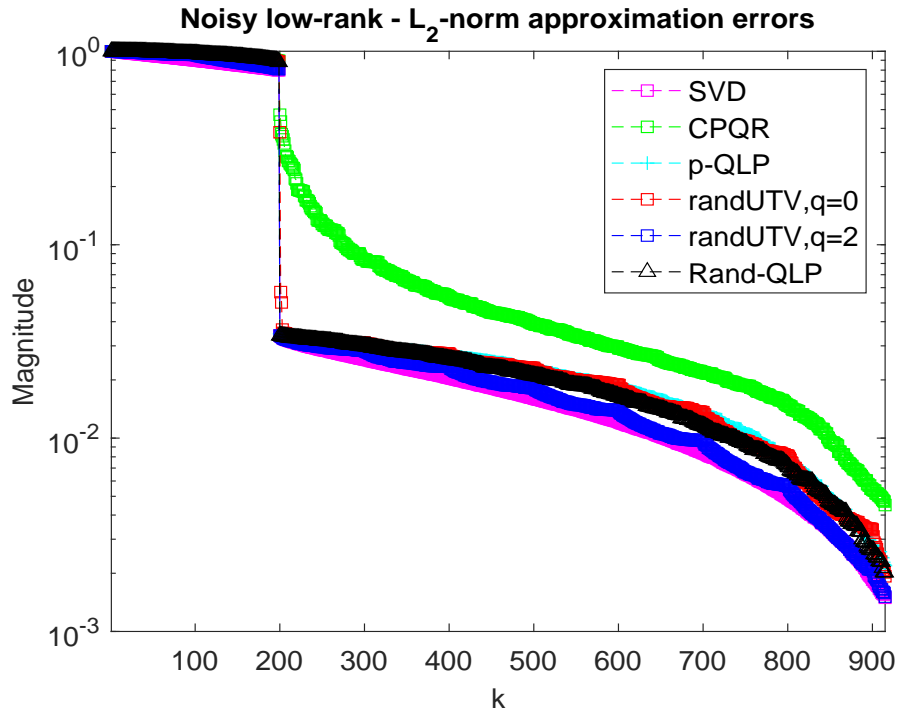
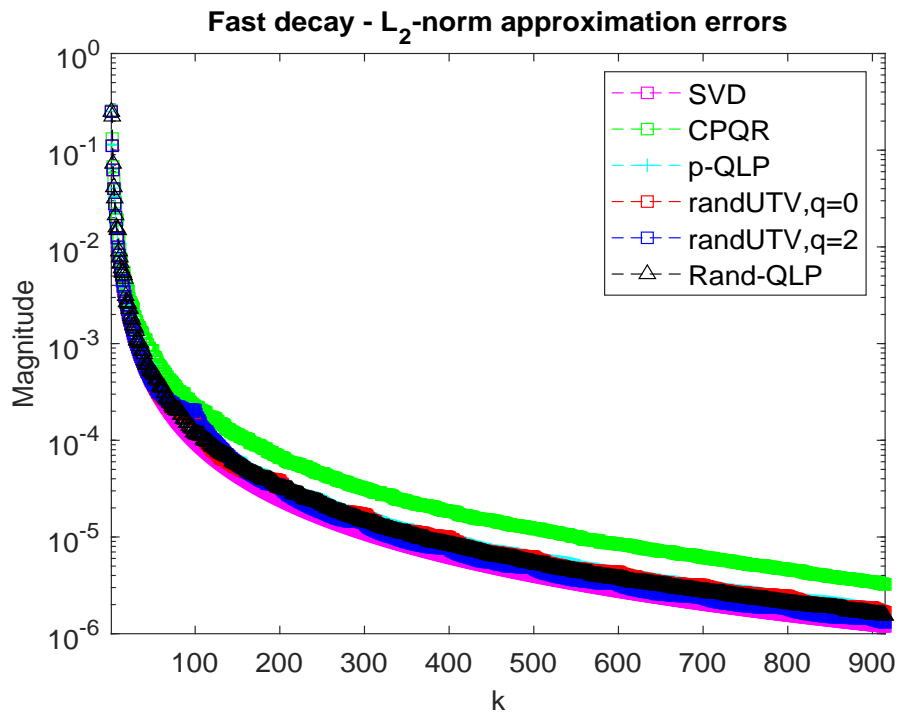


Fig. 4: Singular values approximation.

Fig. 5: Rank- $k$  approximation error.Fig. 6: Rank- $k$  approximation error.

Fig. 7: Rank- $k$  approximation error.Fig. 8: Rank- $k$  approximation error.

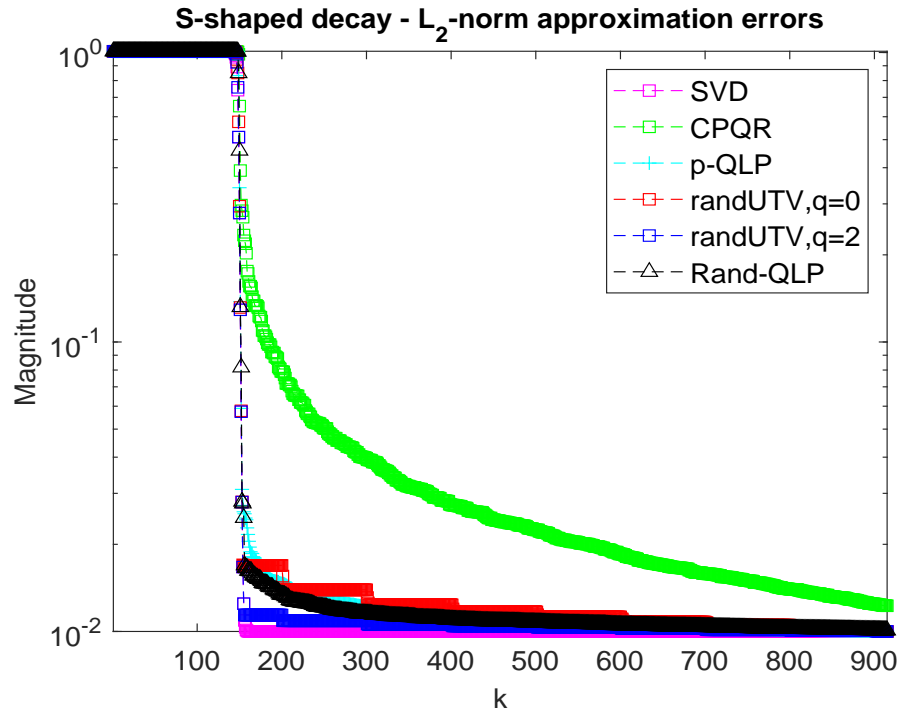
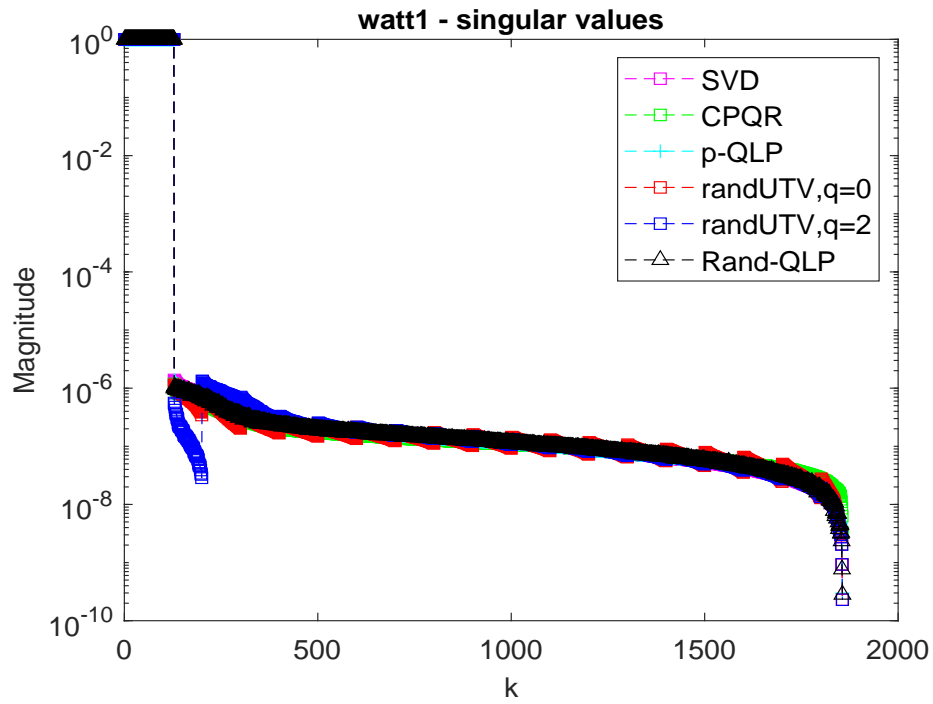
Fig. 9: Rank- $k$  approximation error.

Fig. 10: Singular values approximation.

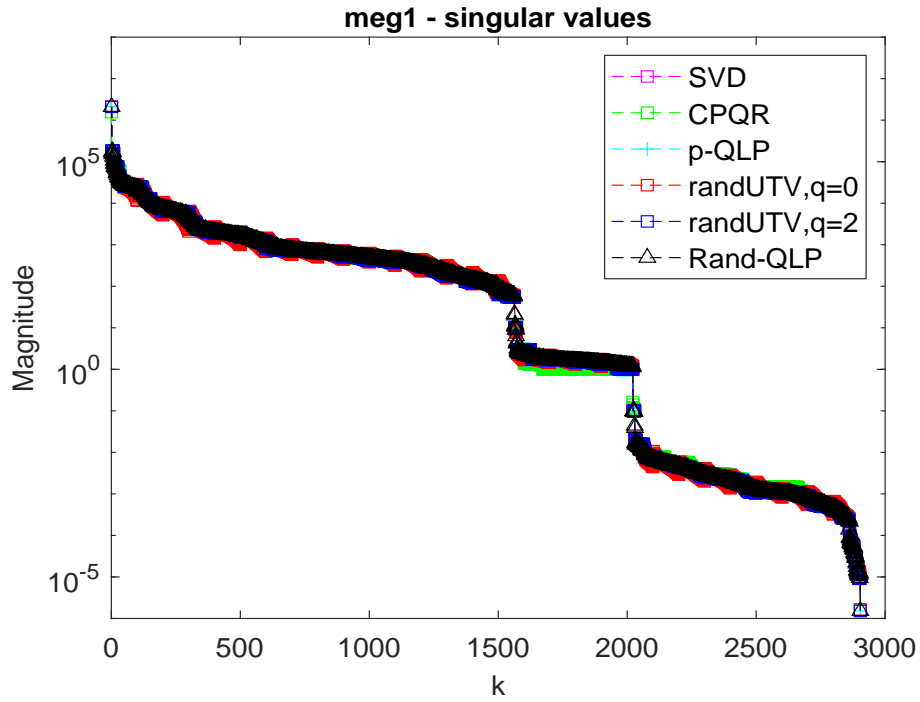


Fig. 11: Singular values approximation.

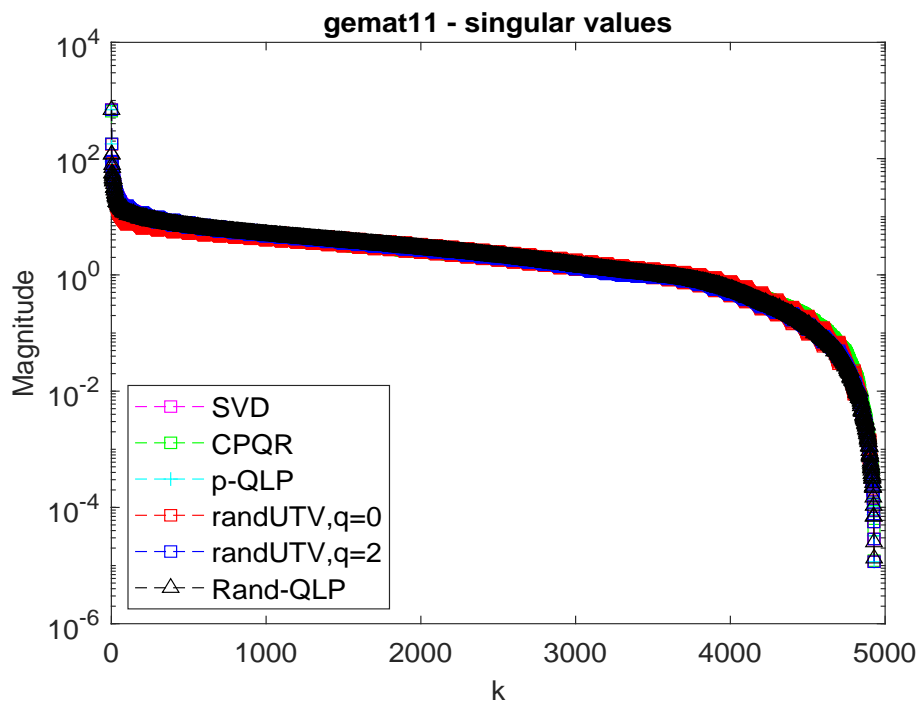


Fig. 12: Singular values approximation.

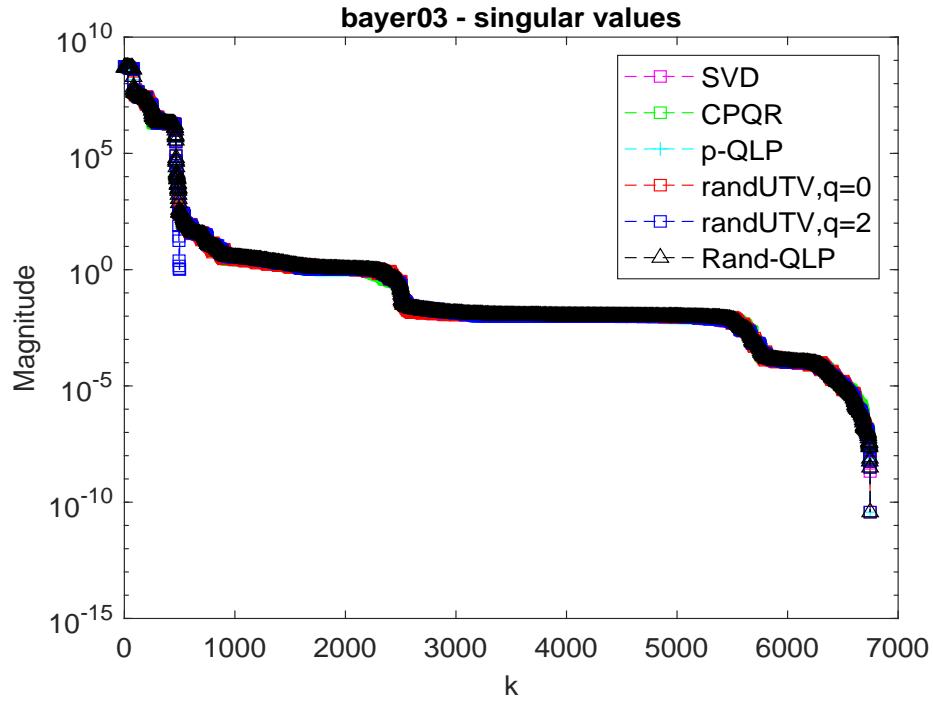


Fig. 13: Singular values approximation.

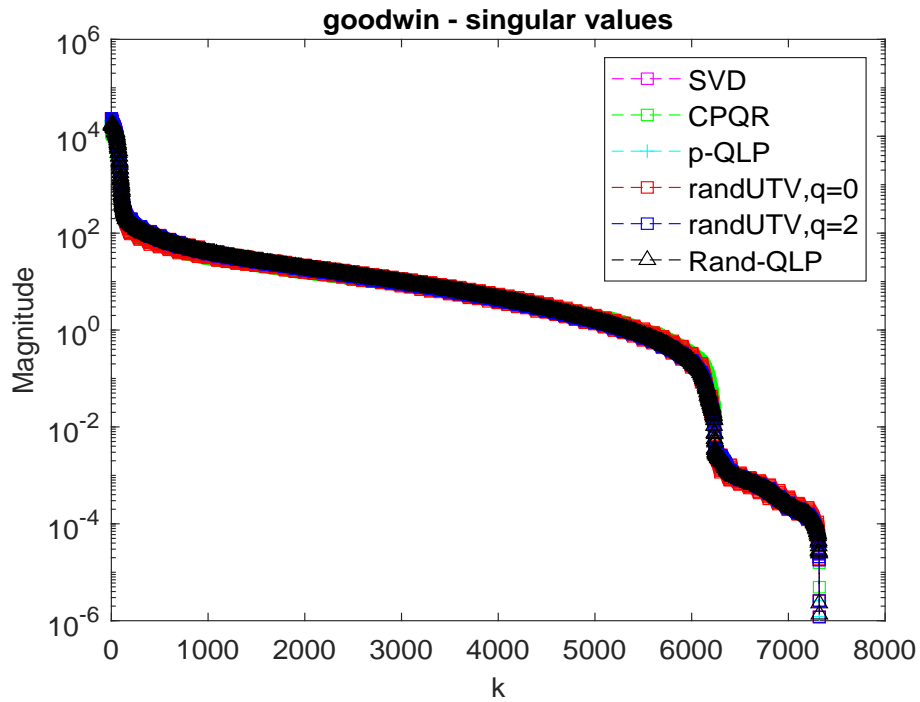


Fig. 14: Singular values approximation.

## REFERENCES

- [1] I. T. Jolliffe, *Principal component analysis*. 2nd ed.: Springer, 2002.
- [2] A. Björck, *Numerical methods for least squares problems*. SIAM, 1996.
- [3] S. Foucart, D. Needell, R. Pathak, Y. Plan, and M. Wootters, “Weighted matrix completion from non-random, non-uniform sampling patterns,” *IEEE Trans. Inf. Theory*, vol. 67, no. 2, pp. 1264–1290, Feb 2021.
- [4] M. F. Kaloorazi and J. Chen, “Efficient low-rank approximation of matrices based on randomized pivoted decomposition,” *IEEE Trans. Signal Process.*, vol. 68, pp. 3575–3589, Jun 2020.
- [5] F. Gygi, “Architecture of Qbox: A scalable first-principles molecular dynamics code,” *IBM Journal of Research and Development*, vol. 52, pp. 137–144, Jan 2008.
- [6] R. de Lamare and R. Sampaio-Neto, “Adaptive reduced-rank processing based on joint and iterative interpolation, decimation, and filtering,” *IEEE Trans. Signal Process.*, vol. 57, no. 7, pp. 2503–2514, 2009.
- [7] R. W. Freund, “Model reduction methods based on Krylov subspaces,” *Acta Numerica*, vol. 12, pp. 267–319, Jul 2003.
- [8] M. F. Kaloorazi and R. C. de Lamare, “Subspace-orbit randomized decomposition for low-rank matrix approximations,” *IEEE Trans. Signal Process.*, vol. 66, no. 16, pp. 4409–4424, Aug 2018.
- [9] G. Unger, “Convergence orders of iterative methods for nonlinear eigenvalue problems,” *Apel T., Steinbach O. (eds) Advanced Finite Element Methods and Applications. Lecture Notes in Applied and Computational Mechanics, Springer, Berlin, Heidelberg*, vol. 66, 2013.
- [10] J. Chen, C. Richard, and A. H. Sayed, “Multitask diffusion adaptation over networks with common latent representations,” *IEEE J. Sel. Topics Signal Process.*, vol. 11, no. 3, pp. 563–579, Apr 2017.
- [11] A. Roy, B. L. Dowdell, and K. J. Marfurt, “Characterizing a Mississippian tripolitic chert reservoir using 3D unsupervised and supervised multiattribute seismic facies analysis: An example from Osage county, Oklahoma,” *Interpretation*, vol. 1, pp. SB109–SB124, Oct 2013.
- [12] M. F. Kaloorazi and R. C. de Lamare, “Anomaly detection in IP networks based on randomized subspace methods,” in *ICASSP, USA*, Mar 2017, pp. 4222–4226.
- [13] G. H. Golub and C. F. van Loan, *Matrix computations*, 3rd ed., Johns Hopkins Univ. Press, Baltimore, MD, 1996.
- [14] T. F. Chan, “Rank revealing QR factorizations,” *Linear Algebra and its Applications*, vol. 88–89, pp. 67–82, Apr 1987.
- [15] G. Stewart, “An updating algorithm for subspace tracking,” *IEEE Trans. Signal Process.*, vol. 40, no. 6, pp. 1535–1541, Jun 1992.
- [16] G. W. Stewart, “Updating a rank-revealing ULV decomposition,” *SIAM J. Matrix Anal. & Appl.*, vol. 14, no. 2, pp. 494–499, 1993.
- [17] P. C. Hansen, *Rank-deficient and discrete ill-posed problems: Numerical aspects of linear inversion*, SIAM, Philadelphia, PA, USA, 1998.
- [18] G. W. Stewart, “The QLP approximation to the singular value decomposition,” *SIAM J. Sci. Comput.*, vol. 20, no. 4, pp. 1336–1348, 1999.
- [19] J. Demmel, L. Grigori, M. Gu, and H. Xiang, “Communication avoiding rank revealing QR factorization with column pivoting,” *SIAM J. Matrix Anal. & Appl.*, vol. 36, no. 1, pp. 55–89, 2015.
- [20] C. L. Lawson, R. J. Hanson, D. R. Kincaid, and F. T. Krogh, “Basic linear algebra subprograms for FORTRAN usage,” *ACM Transactions on Mathematical Software (TOMS)*, vol. 5, pp. 308–323, 1979.
- [21] J. Dongarra, J. Du Croz, S. Hammarling, and R. J. Hanson, “An extended set of FORTRAN basic linear algebra subprograms,” *ACM Transactions on Mathematical Software (TOMS)*, vol. 14, pp. 18–32, 1988.



- [22] J. Dongarra, J. Du Croz, S. Hammarling, and I. S. Duff, "A set of level 3 basic linear algebra subprograms," *ACM Transactions on Mathematical Software (TOMS)*, vol. 16, pp. 1–17, 1990.
- [23] J. Dongarra, M. Gates, A. Haider, J. Kurzak, P. Luszczek, S. Tomov, and I. Yamazaki, "The singular value decomposition: Anatomy of optimizing an algorithm for extreme scale," *SIAM Rev.*, vol. 60, no. 4, p. 808–865, 2018.
- [24] M. F. Kaloorazi and J. Chen, "Projection-based QLP algorithm for efficiently computing low-rank approximation of matrices," *IEEE Trans. Signal Process.*, vol. 69, pp. 2218–2232, Mar 2021.
- [25] L. N. Trefethen and D. Bau III, *Numerical linear algebra*, SIAM, 1997.
- [26] R. D. Fierro and P. C. Hansen, "Low-rank revealing UTV decompositions," *Numerical Algorithms*, vol. 15, no. 1, pp. 37–55, Jul 1997.
- [27] G. Quintana-Ortí, X. Sun, and C. H. Bischof, "A BLAS-3 version of the QR factorization with column pivoting," *SIAM J. Sci. Comput.*, vol. 19, no. 5, pp. 1486–1494, 1998.
- [28] Y. Nakatsukasa and N. Higham, "Stable and efficient spectral divide and conquer algorithms for the symmetric eigenvalue decomposition and the SVD," *SIAM J. Sci. Comput.*, vol. 35, no. 3, p. A1325–A1349, 2013.
- [29] N. Higham, *Functions of matrices: theory and computation*, SIAM, Philadelphia, 2008.
- [30] P. Martinsson, G. Quintana-Ortí, and N. Heavner, "randUTV: A blocked randomized algorithm for computing a rank-revealing UTV factorization," *ACM Trans. Math. Softw.*, vol. 45, no. 1, pp. 4:1–4:26, Mar. 2019.
- [31] T. Davis and Y. Hu, "The University of Florida Sparse Matrix Collection," *ACM Trans. Math. Softw.*, vol. 38, no. 1, pp. 1–25, 2011.
- [32] G. Stewart and J. Sun, *Matrix Perturbation Theory*, Academic Press, 1990.
- [33] H. Henderson and R. Searle, "On Deriving the Inverse of a Sum of Matrices," *SIAM Rev.*, vol. 23, no. 1, pp. 53–60, 1981.